NUMERICAL DESIGN PARAMETER STUDY FOR SLOTTED WALLS IN TRANSONIC WIND TUNNELS

ICAS-86-1.6.2

Nada Agrell, Björn Pettersson
FFA, The Aeronautical Research Institute of Sweden, S-161 11 BROMMA, Sweden
and
Yngve C-J. Sedin
SAAB-SCANIA AB, S-581 88 Linköping, Sweden

Abstract

A method using local slot boundary conditions has been applied for design and analysis of optimal slots giving minimum or very low wall interference in transonic wind tunnels with slotted walls. The basically inviscid mathematical model was corrected for viscid effects. The considered test section is rectangular and the flow inside was computed using the nonlinear transonic small perturbation equation. Separate equations were solved for each slot. Encouraging results have been obtained for a relatively large wing-body model at two Mach numbers and at two angles of attack. The set of slot shapes designed for these flight conditions were computationally verified to give low interference on the test model. The inverse design mode gave the necessary slot geometries and the plenum pressure. Direct mode calculations then gave the wall interference and in principle also the mass flow setting of the tunnel.

Introduction

The cost of wind tunnel facilities and testing is increasing with linear dimensions of the tunnel. This can be prevented by running bigger models in tunnels equipped by active walls to reduce the wall interference. An interesting application of this is e.g. shown by Ganzer[1], where flexible walls for a 3D high speed tunnel are demonstrated.

The present method represents a somewhat different approach to get low interference. It investigates the possibilities of using optimally designed slots in plane tunnel walls, that can be slightly inclined against the tunnel axis, typically 0-1 degrees of inclination, depending on the lift. So far, the investigations have been of computational nature only, although the slot flow model as such has been verified by Sedin and Sörensen[2] comparing computations with experiments carried out at The Aero nautical Research Inst. of Sweden (FFA).

The outcome of the present investigation is a set of slot geometries at a number of flight conditions for which the wall interference has been confirmed to be very low for a relatively big wind tunnel model, blocking about 1.5 % of the test section.

The software system developed for the present investigation has mainly been composed by parts earlier developed by Karlsson-Sedin[3-4], and Sedin-Agrell-Zhang[5]. The local slot boundary condition has been developed in Ref. 5, while the optimal slot design has basically been described in Ref. 3. The slot flow model is the same as developed by Berndt[6]. The viscous corrected theory is a simplified version of that developed by Sedin[2].

The computations have mainly been carried out on a CRAY-1A supercomputer. In the following the mathematical and physical formulations in terms of equations will be kept to a minimum. Interested readers are referred to the given list of references.

Slot flow model

The slot flow is schematically shown in Fig. 1. The physical model is basically inviscid and based on a 2D cross-flow theory. The viscous correction is included via two reduction factors, η_a for the slot width a(x) and η_u for the axial velocity U. Typical values for these factors can be 0.6-0.8, see Ref. 2. These loss factors are assumed to be constants.

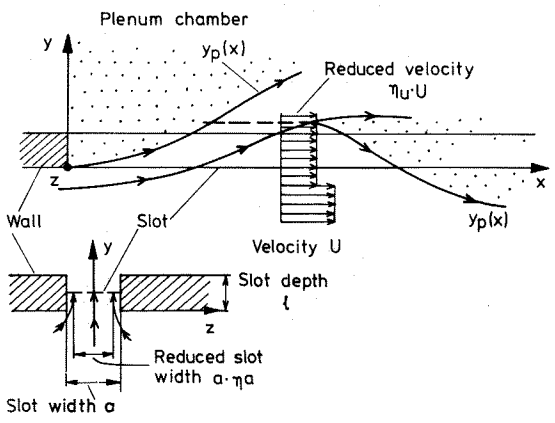

Fig. 1 Slot flow model.

The slot flow equations consist of two relations, one to determine the plenum pressure surface yp(x) and the other gives the pressure difference across the slot in terms of the slot flux q(x) per unit length, the slot width a(x) and the plenum surface position yp(x). The slot flux q is a priori unknown and must be determined as a part of the total solution including the interaction with the interior test section flow generated by the wind tunnel model.

The plenum surface position yp(x) and the pressure equation are evaluated in the slot centreplane z=0. The xyz-syst is a local slot coordinate system, see Fig. 1. Symbolically, we may write the slot flow equations:

$$yp'(x) = f(q(x),a(x),a'(x),yp(x)) \quad (1)$$

$$F(q(x),a(x),a'(x),a''(x),yp'(x)) + \phi_x(x,0,0) + \delta = 0 \quad (2)$$

where f and F are short hand for functional relations and ',' indicate 1st and 2nd order derivatives respectively. The $\phi_x(x,0,0)$ in Eq.(2) is the disturbance velocity of the approximate interior test section problem and δ denotes the normalized plenum pressure coefficient, see e.g. Ref. 6. Eq.(2) is the integrated cross-flow part of the momentum equation in the slot centre plane and generates the wall boundary condition on the wall strips for the test section flow. For a discussion, see Refs. 2 and 5. Not explicitly shown in Eq.(2) is the slot flow reduction due to viscous effects (see Fig. 1 and also Ref. 2), the factors η_u and η_a. Using these, the effective axial velocity will approximatly be $\eta_u U_\infty$ and the effective slot width $\eta_a a$. An estimation of the corresponding mass density in the slot flow region is found by assuming constant total enthalpy. U_∞ is the reference velocity 'labelled' by the nominal reference Mach number M_∞ for the tunnel run.

Outer field equation and boundary conditions

The field equation for the approximate problem, away from the slots in the test section, is given by the nonlinear small perturbation potential equation:

$$(1-M_\infty^2 - (\gamma+1)M_\infty^2\phi_x)\phi_{xx} + \phi_{yy} + \phi_{zz} = 0 \quad (3)$$

Here ϕ is the disturbance potential, M_∞ the nominal reference Mach number labelling the tunnel run and U_∞ the corresponding reference velocity normalized to 1. γ is the specific heat ratio, $\gamma=1.4$ for air. In Eq.(3) x,y,z is a fixed Cartesian system with x pointing downstream in the direction of the tunnel axis.

Conventional no-through-flow conditions are imposed on the wind tunnel test model, while the wall boundary conditions for Eq.(3) are of mixed Neumann-Dirichlet type, as schematically shown in Fig. 2. Hence, on the walls between the slot strips (as many as the slots but wider) the normal velocities are given by the turbulent wall boundary layer displacement thickness and the existing wall inclination. On the slot strips a local slot boundary condition, as developed in Ref. 5, is applied giving $\phi(x,0,z)$ in terms of the slot flux (see Fig. 2). The slot flux q is found through a mass flux balance for each slot, approximately yielding

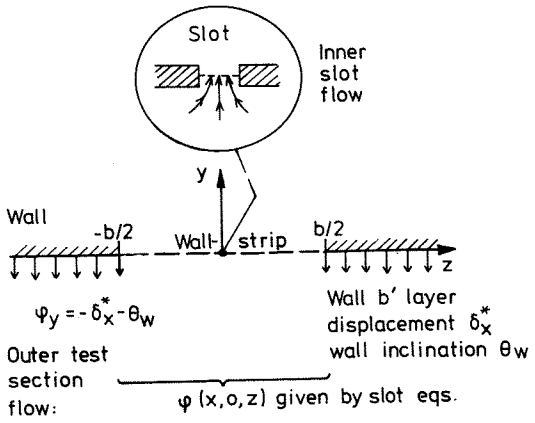

Fig. 2 Local slot boundary condition.

$$q = \int_{-b/2}^{b/2} \phi_y \, dy + b(\delta_x^* + \theta_w) \quad (4)$$

Here b is the strip width, δ_x^* the displacement thickness gradient and θ_w the wall inclination. The contribution from the interior flow is the integral part of Eq.(4). Equation (4) couples the interior of the test section, Eq.(3), to the slot flow described by Eqs(1) and (2). In Fig. 2 x,y,z are local strip coordinates with z=0, y=0 in the middle of the strip.

On the solid wall between the wall strips the Neumann condition reads (with the y-axis pointing in the outward direction, see Fig. 2):

$$\phi_y(x,0,z) = -\delta_x^* - \theta_w \quad (5)$$

The Dirichlet condition on the wall strips reads:

$$\phi(x,0,z) = D(\phi(x,0,0)) \quad (6)$$

where D is a special distribution function, see Ref. 5, and $\phi(x,0,0)$ is obtained from the slot flow Eq.(2). The slot flow and the test section flow are coupled by matched asymptotic expansion. Hence, Eqs.(4) and (6) are the important relations knitting together the inner slot flow with the outer (interior) test section flow for each slot.

On the inflow-plane of the test section a quadratic distribution function for ϕ is assumed, leading to $\phi=0$ in the middle of the test section. The coefficients of the quadratic approximation are determined by fulfilling the normal velocities on the walls. Hence, with this formulation, the disturbance velocity ϕ_x at the inflow-plane will be a natural outcome of the interior field computation and can be used to define the natural mass flow setting of the test section. It might look paradoxal that this flux parameter is not in hand

from the very beginning. However, qualitatively in transonic flow, the cross-flow through the slots is approximately determined by the geometry of the test model only. Hence, the pressure difference across the slot will be almost independent of Mach number. A consequence of this will then be that the level of the pressure distribution (ϕ_x) inside the test section is determined by the chosen plenum pressure and model geometry only. Hence, a mismatch could occur at the inflow section if one tries to specify ϕ_x there, unless this is the natural and correct value for a possible smooth test section flow at the upstream inflow-plane. This type of difficulty was numerically detected in Ref. 3.

In summary, Eqs.(1)-(6) constitute the closed nonlinear system that has to be solved by an iterative technique, repeatedly updating the boundary conditions of Eq.(3) in the direct (analysis) computational mode.

Eq.(3) was numerically solved using a conventional relaxation technique[7], while the slot flow Eqs.(1)-(2) were solved using a predictor-corrector scheme[3].

Optimal slot design procedure

The first step in the optimal slot design procedure is to solve the desired unbounded freestream case using the small perturbation potential equation (Eq.(3)). The second step is to estimate the individual mass fluxes (Eq(4)) through each slot. This is obtained by distributing the disturbance potential from step one along wall strips and then solving for the test section flow (Eq.(3)) with a no through-flow condition applied between the strips, Fig.2. The required pressure difference between the plenum chamber and the (interference-free) interior of the test section is used in step three to solve each slot shape (Eqs.(1)-(2)). The "interference-free" pressure should be obtained just outside the immediate vicinity of the slot, close to the wall in the test section. When integrating Eq.(2) with respect to the slot width a(x), velocity ϕ_x is used as calculated at the imagined slot position for the freestream case.

For cases with an angle of attack it was found necessary to apply a slight wall inclination to compensate for the downwash. However, this inclination could be kept constant for all slots in the considered wall simplifying practical design considerations.

Once the above procedure has been successfully terminated, resulting in a set of slot shapes and an adequate plenum chamber pressure, an analysis mode calculation has to be performed. This in order to compute the integrated total mass flux entering the test section as well as to check how small the wall interference really is. The corresponding tunnel setting is then defined by the mass flow and the plenum chamber pressure. With this setting an almost interference-free situation should appear for the test model at the desired freestream Mach number. The present results seem to indicate that the total forces, lift-, drag and pitching moment, will be reproduced within a couple of percent compared to the desired unbounded freestream case, even for unusually big models.

In order to save computer and preparation time, work is in progress to shortcut step two in the optimal design mode above and direcly go from the step one (freestream) to the step three (optimal slot design) procedure.

In summary, the following flow chart can be outlined for the present slot design procedure:

1) Solve for the desired freestream case, Eq.(3).

2) Estimate the slot fluxes q, Eq.(4), by solving an approximate problem, Eq.(3), using ϕ from 1)along the wall strips, Fig. 2.

3) Guess plenum pressure and slot depth (and wall inclination if necessary). Integrate slot flow Eqs(1)-(2) with respect to the slot shape a(x) using q from 2) and $\phi(x,0,0)$ from 1).

4) If 3) is successfully terminated with a physical slot shape then go to 5) else go to 3) and repeat with new input data.

5) Check the wall interference by a direct (analysis) mode calculation using the slots obtained in 3).

6) If the outcome of 5) is satisfactory, the tunnel setting will be given by the current plenum pressure and the test section mass flow as integrated from step 5)

Convenient slot shapes are usually found within a few attempts in the iterative loop.

Numerical computations

The considered test section with model is shown in Fig. 3. The tunnel dimensions are $14\times5\times5$ dm^3. It is provided by 8 slots. A slot of standard shape, the same for all walls, is also illustrated. The wind tunnel model has got a delta wing of 5% relative thickness which together with the axisymmetric body will give a blockage ratio of about 1.5% in the test section.

For simplicity, only one 2D viscous turbulent wall boundary layer is considered for each wall. The pressure gradi-

ents at positions A, B and F are driving the boundary layer integral momentum equation. Concerning the viscous slot flow losses the values η_a=0.7 and η_u=0.7 have been used in all calculations. The Reynolds' number per unit length was $1.48 \cdot 10^6$ and the wall boundary layer thickness at the beginning of the test section was set to 0.35 dm.

In the following, the set of optimal slots will be given names like M95A5 meaning that the design Mach number and angle of attack have the values 0.95 and 5 degrees, respectively. Moreover the wall inclinations of the top, bottom and side walls will be denoted by Θ_{w_t}, Θ_{w_b} and Θ_{w_s} respectively. The plenum pressure coefficient δ is defined to be half the conventional C_p in the plenum chamber ($\delta = C_p/2$). The symbol l is the slot depth. The noted ventilation in % is the wall ventilation when considering all the 8 slots together at the model position. The wall inclinations are expressed in degrees. A positive inclination of the walls means a 'converging' tunnel.

Some data for the calculated slots can be found in Table 1:

Some overall information about the computed wall interference in terms of interference numbers is shown in Table 2. The interference is quantified using relative numbers called Figures of Tunnel Interference: for the lift FTIL, for the drag FTID and for the pitching moment FTIM, respectively. These numbers are defined according to:

$$FTIx = ((x)_t - (x)_f)/(x)_f \quad ,$$

where index t indicates tunnel data and index f unbounded freestream data.

Mach number M_∞ is the nominal reference value that labels the tunnel run. This Mach number is usually defined through calibrated data in an empty test section. However, this kind of procedure will in principle be useless when using big models. In such cases other methods must be used to define a 'valid' freestream Mach number and to give the proper tunnel setting. In this matter a computational method like the present will be of great value.

From Table 2 it can be seen how the optimally designed slots give low interference at design and are reasonably good also at off-design conditions.

For low transonic Mach numbers the interference is not specially sensitive with respect to the slot shapes. This can be seen in Table 2 for the standard slot at M_∞=0.70.

The optimal design procedure together with the subsequent direct mode calculation (tunnel run) will define the tunnel setting in terms of the incoming mass flux at the upstream inflow section, the pressure in the plenum chamber and wall inclinations as well. Hence, in a real tunnel run, these data should be strived for using the designed slot geometries and wall inclinations.

Comments on the numerical results

In Figs. 4-5 the interference situation using the standard slots is shown at the nominal M_∞ = 0.95 and α = 5 degrees. The shock on the wing is not in the right position compared to the freestream 'target' and the compression on the top wall at position B in front of and behind the wing is too strong and the pressure level is too high at the wing position. This mismatch compared with the desired freestream case is partly due to a too small ventilation.

According to Figs. 6 and 7 a great improvement is found using the optimal slots M95A5 compared to the standard slots for the same nominal freestream condition. Looking at Fig. 6, the pressures along two spanwise stations on the wing (see Fig. 3) almost lie on top of the desired freestream data. A good agreement is also found in Fig. 7 concerning the wall pressures along A, B and F (see Fig. 3). However, there is a pronounced disagreement in wall pressures compared to the freestream case at the inflow section. This is due to the wall inclination, that was required (see Table 1), as well as the wall boundary layer. A mean value of the gradient (acceleration) ϕ_{xx} can easily be estimated by applying Green's identity to Eq.(3) in cross-flow planes, also taking into account the slot fluxes q. Such an analysis clearly shows how the gradient ϕ_{xx} falls off further downstream when the q's are getting positive (corresponding to slot inflow conditions) striving to overcome the converging effects of the positive wall inclinations.

In Fig. 8 comparisons are made between the optimal slots M95A5 and the standard slots at M_∞= 0.95 and α = 5 degrees for slot number 2. Slots in the top wall are usually critical concerning the need for wall inclinations due to the downwash behind a wing with lift. This is reflected in the graph for the plenum pressure position yp(x) of the standard slot. For this slot yp(x) becomes negative at the aft part of the wind tunnel model, indicating that a bubble of quiscent plenum air is expanding into the test section creating interference. One measure against this would be to make the standard slot more efficient by increasing the slot depth. Another possibility to prevent the backflow behaviour could be to apply some wall inclination. Still another would be to increase the slot width for the standard slot, a conclusion that can be drawn by looking at the optimal slot width of M95A5.

Figure 9 is showing the complete set of optimal slots M95A5. Wall inclinations were necessary for all walls except for the bottom wall. Generally the character of the slot geometries, considering bottom, side and top walls, is changing due to the flow asymmetry imposed by the lift. Due to different wall inclinations (see Table 1) for bottom and side walls the slot widths of slot 1 and slot 3 are also different, while slots 2 and 4 are quite similar because of the fact that both top and side walls have got the same wall inclination. Another interesting feature that can be observed in Fig. 9 is the rapid almost step like increase in slot width for slots 3, 4 and 2 at about x=9.5. This is caused by the local increase in the boundary layer displacement thickness which is a consequence of the steep positive wall pressure gradient.

Figure 10 is showing the set of slots M70A5, designed for M_∞=0.70 and α=5 deg. The shapes of these slots do not differ very much from M95A5 giving good hope for pleasant off-design behaviours in the Mach number regime for the specified model and angle of attack.

Figures 11 and 12 show wing and wall pressure distributions for slots M70A5. These calculations confirm the low interference that can be obtained. The disagreement in wall pressure at the inflow section is also present for this set of slots. The previous explanation is of course valid here too. A certain dicrepancy can also be found in the wall pressure above the model. However, this does not seem to affect the good agreement on the wing itself (Fig. 11 and Table 2).

Figures 13 and 14 illustrate crosswise off-design calculations, computed at M_∞=0.70 with slots M95A5 and at M_∞=0.95 with slots M70A5 at 5 degrees angle of attack. As can be seen from Figs. 13, 14 and Table 2 there is an increase in interference compared to the respective design points. However, the deteriorations stay within a couple of percent for the most sensitive M95A5 slots. This is probably due to a more severe influence of the wall boundary layer on the slot design at higher design Mach numbers. This emphazises the importance of wall boundary layers in transonic tunnels, especially, when strong shocks are striking the walls and boundary layer separation occurs.

Finally Figs. 15 and 16 show optimally designed slots at zero angle of attack for Mach numbers 0.70 (M70A0) and 0.95 (M95A0). It is interesting to see how similar all slots within one set are reflecting the almost axisymmetric flow that is asymptotically generated far away from the wind tunnel model. Direct mode calculations in the design points have confirmed very low interference numbers for the above slot shapes at zero angle of attack. As there is no asymmetric flow due to lift no wall inclinations have been necessary.

Concluding remarks

A method has been developed for the purpose of numerical design and analysis of slotted walls for rectangular test sections of transonic wind tunnels using individual simulation of the slot flows. Encouraging results have been obtained for a relatively big model giving low wall interference for a number of numerical test cases. The present method can give important contributions to the understanding of physical parameters of importance in slotted wall test sections. The physical and mathematical models including qualitative viscous effects are simple enough for repeated use on high speed computers.

An experimental verification of the slotted wall design procedure has yet to be performed. Once this has been done, it should be possible, by using the present method, to design slotted wall test sections for much bigger test models than used hitherto.

References

1 Ganzer, U.: Über Messungen im hohen Unterschall in dem Windkanal der TU-Berlin mit adaptiven Wänden, 4. BMFT-Statusseminar, Luftfahrtforschung und Luftfahrttechnologie, April 1986.

2 Sedin, Y.C-J. and Sörensen, H.: Computed and Measured Wall Interference in a Slotted Transonic Test Section, AIAA J. Vol. 24, March 1986, pp. 444-450.

3 Karlsson, K.R. and Sedin, Y.C-J.: Numerical Design and Analysis of Optimal Slot Shapes for Transonic Test Sections-Axisymmetric Flows, Journal of Aircr., Vol. 18, March 1981, pp. 168-175.

4 Sedin, Y.C-J. and Karlsson, K.R.: Some Theoretical Wall-Interference Calculations in Slotted Transonic Test Sections-Three Dimensional Flows, ICAS Proc., Vol. 1, Seattle, Wash., Aug. 1982.

5 Sedin, Y.C-J., Agrell, N. and Zhang, N.: Computation of Transonic Wall-Interference in Slotted-Wall Test Sections of Wind Tunnels, ISCFD, Tokyo, Sept 1985.

6 Berndt, S.B.: Inviscid Theory of Wall Interference in Slotted Test Sections, AIAA J. Vol. 15, Sept 1977, pp. 1278-1287.

7 Agrell, N. and Hedman, S.G.: Calculations of Transonic Steady State Aeroelastic Effects for a Canard Airplane, ICAS Proc., Vol. 1, Seattle, Wash., Aug. 1982

Table 1 Data for calculated cases.

Slot	M_{des}	max vent. %	ℓ	Plenum C_p	Θ^o top-wall	Θ^o bottom-wall	Θ^o side-wall
Stand	0.70	5.7	0.07	0.0	0.	0.	0.
-"-	0.95	5.7	0.07	0.0	0.	0.	0.
M70A5	0.70	17.5	0.8	-0.01	.37	0.	.37
M95A5	0.95	17.9	0.8	-0.01	.37	0.	.37
M70A0	0.70	8.0	0.8	-0.01	0.	0.	0.
M95A0	0.95	8.8	0.8	-0.01	0.	0.	0.

Table 2 Wall interference numbers.

Fig	Slot	M_∞	α^o	FTIL %	FTIM %	FTID %
-	Standard	0.70	5	0.5	-1.0	0.0
4-5	-"-	0.95	5	-8.4	-13.5	15.1
6-7	M95A5	0.95	5	1.7	2.0	0.0
13	M95A5	0.70	5	-2.7	-4.4	-2.1
11-12	M70A5	0.70	5	-0.5	-1.6	0.0
14	M70A5	0.95	5	2.2	2.7	0.9

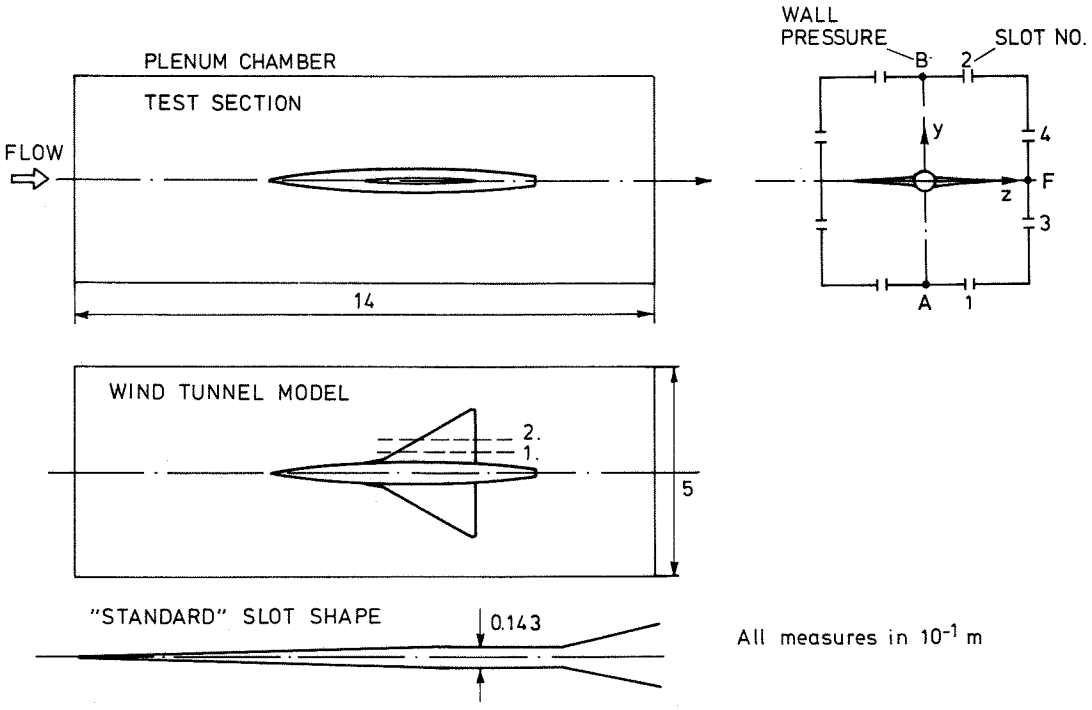

Fig. 3 Test section with model.

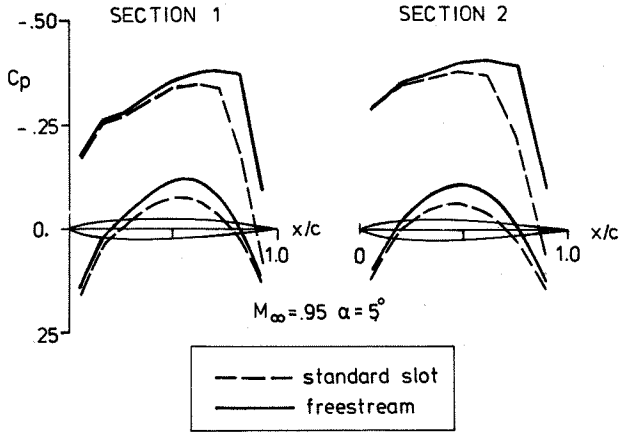

Fig. 4 Wing pressures, standard slot, $M_\infty = 0.95$, $\alpha = 5^o$.

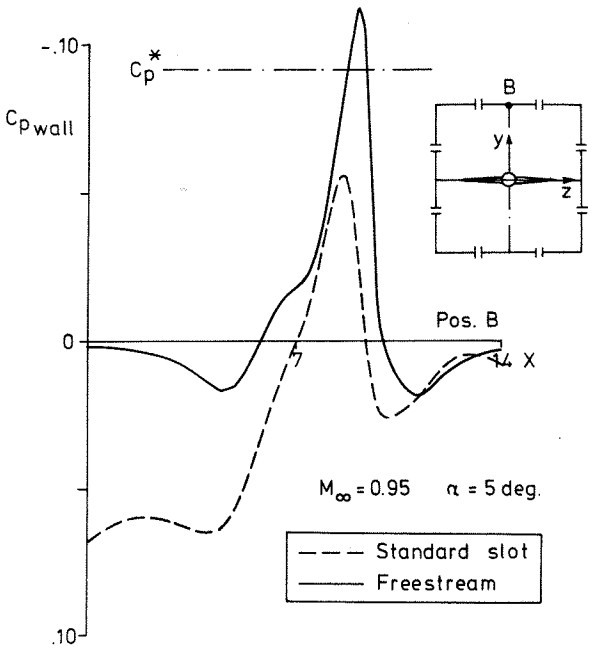

Fig. 5 Wall pressures along line B, standard slot, $M_\infty = 0.95$, $\alpha = 5^o$.

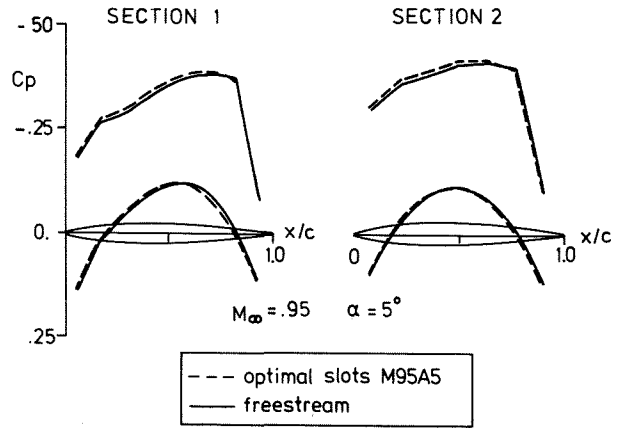

Fig. 6 Wing pressures, optimal slots M95A5, $M_\infty = 0.95$, $\alpha = 5^\circ$.

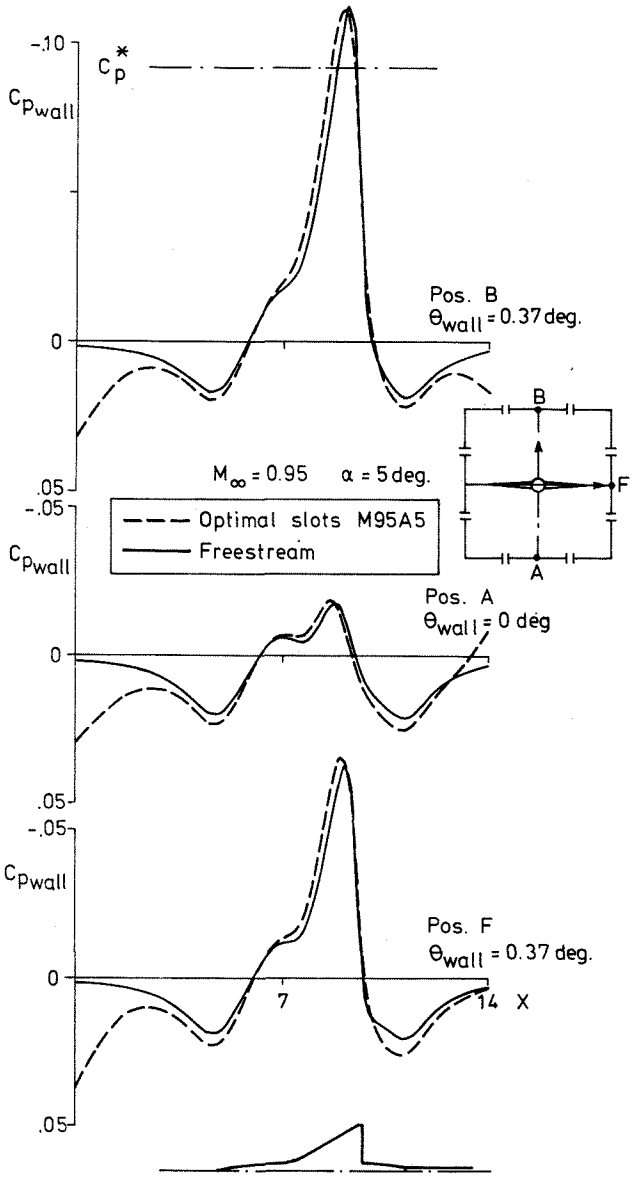

Fig. 7 Wall pressures at pos. B,A,F. Optimal slots M95A5, $M_\infty = 0.95$, $\alpha = 5^\circ$.

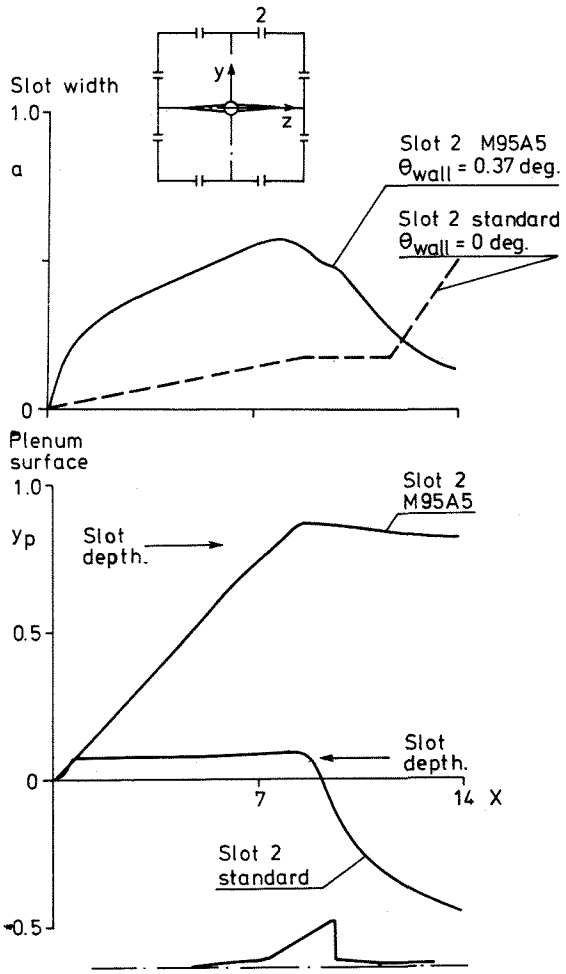

Fig. 8 Slot 2 comparisons: Optimal slot M95A5 and standard slot at $M_\infty = 0.95$, $\alpha = 5^\circ$.

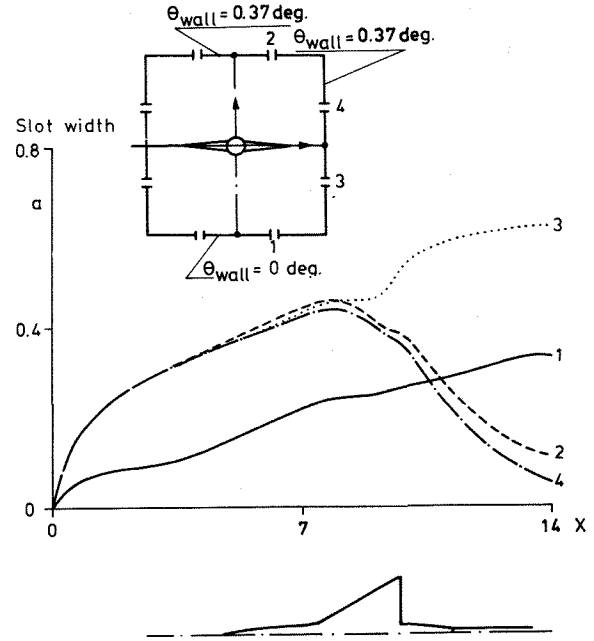

Fig. 9 Optimal slots M95A5 designed for $M_\infty = 0.95$, $\alpha = 5^\circ$.

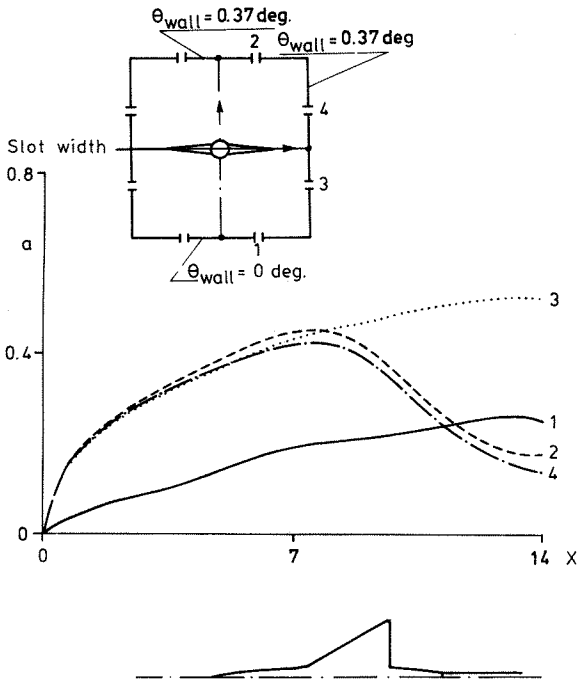

Fig. 10 Optimal slots M70A5 designed for $M_\infty = 0.70$, $\alpha = 5^o$.

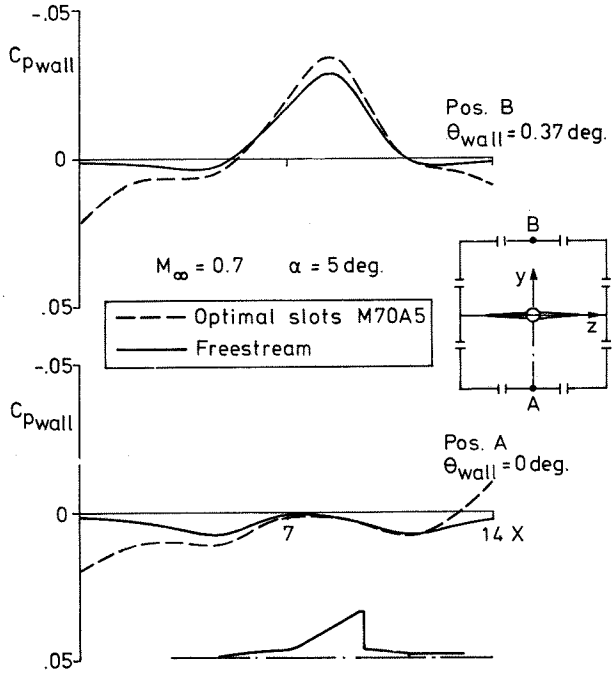

Fig. 12 Wall pressures at pos. A,B. Optimal slots M70A5, $M_\infty = 0.70$, $\alpha = 5^o$.

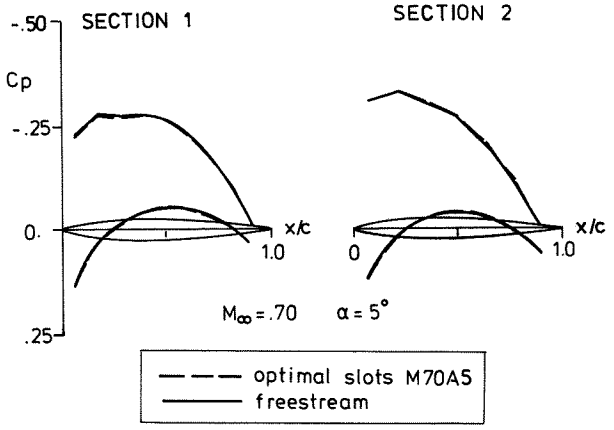

Fig. 11 Wing pressures, optimal slots M70A5, $M_\infty = 0.70$, $\alpha = 5^o$.

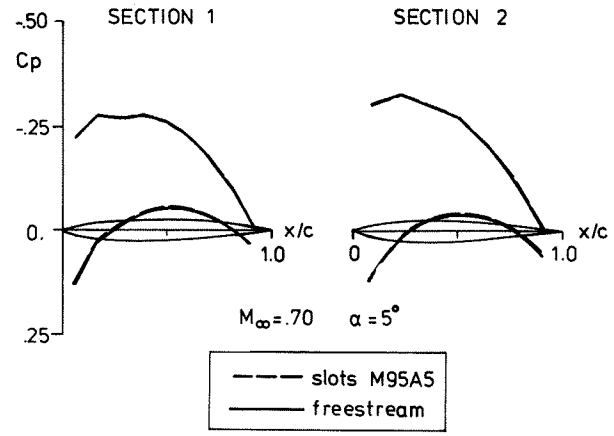

Fig. 13 Wing pressures at off-design. Slots M95A5 at $M_\infty = 0.70$, $\alpha = 5^o$.

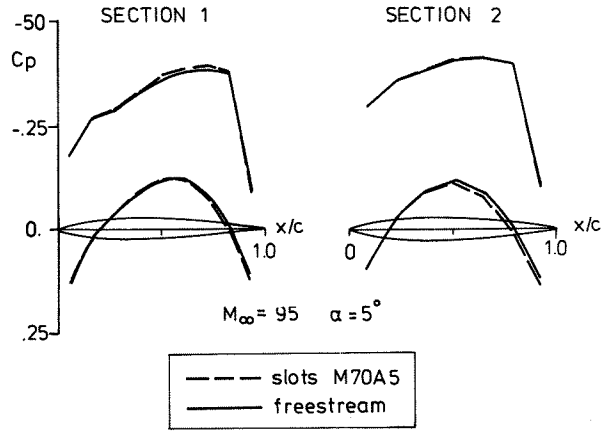

Fig. 14 Wing pressures at off-design. Slots M70A5 at $M_\infty = 0.95$, $\alpha = 5^o$.

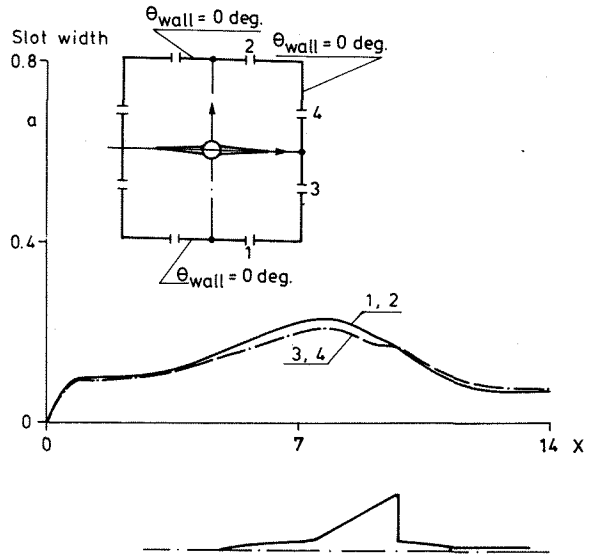

Fig. 15 Optimal slots M95A0 design for $M_\infty = 0.95$, $\alpha = 0^o$.

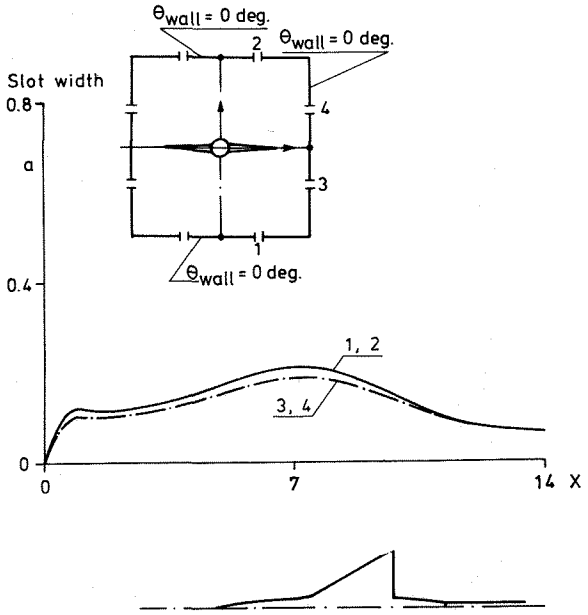

Fig. 16 Optimal slots M70A0 design for $M_\infty = 0.70$, $\alpha = 0^o$.